Tectonophysics 608 (2013) 1298–1309

Contents lists available at ScienceDirect

Tectonophysics

journal homepage: www.elsevier.com/locate/tecto

Length–displacement scaling and fault growth

Agust Gudmundsson [a,*], Giorgio De Guidi [b], Salvatore Scudero [b]

[a] Department of Earth Sciences, Queen's Building, Royal Holloway University of London, Egham TW20 0EX, UK
[b] University of Catania, Department of Biological, Geological and Environmental Sciences, Italy

ARTICLE INFO

Article history:
Received 14 February 2013
Received in revised form 4 June 2013
Accepted 16 June 2013
Available online 26 June 2013

Keywords:
Fault zones
Co-seismic rupture
Fault geometry
Fault damage zone
Fault core
Fault evolution

ABSTRACT

Following an earthquake in a fault zone, commonly the co-seismic rupture length and the slip are measured. Similarly, in a structural analysis of major faults, the total fault length and displacement are measured when possible. It is well known that typical rupture length–slip ratios are generally orders of magnitude larger than typical fault length–displacement ratios. So far, however, most of the measured co-seismic ruptures and faults have been from different areas and commonly hosted by rocks of widely different mechanical properties (which have strong effects on these ratios). Here we present new results on length–displacement ratios from 7 fault zones in Holocene lava flows on the flanks of the volcano Etna (Italy), as well as 10 co-seismic rupture length–slips, and compare them with fault data from Iceland. The displacement and slip data from Etna are mostly from the same fault zones and hosted by rocks with largely the same mechanical properties. For the co-seismic ruptures, the average length is 3657 m, the average slip 0.31 m, and the average length–slip ratio 19,595. For the faults, the average length is 6341 m, the average displacement 73 m, and the average length–displacement ratio 130. Thus, the average rupture–slip ratio is about 150-times larger than the average length–displacement ratio. We propose a model where the differences between the length–slip and the length–displacement ratios can be partly explained by the dynamic Young's modulus of a fault zone being 10^{1-2}-times greater than its static modulus. In this model, the dynamic modulus controls the length–slip ratios whereas the static modulus controls the length–displacement ratio. We suggest that the common aseismic slip in fault zones is partly related to adjustment of the short-term seismogenic length–slip ratios to the long-term length–displacement ratios. Fault displacement is here regarded as analogous to plastic flow, in which case the long-term displacement can be very large so long as sufficient shear stress concentrates in the fault.

1. Introduction

Faults are complex systems whose growth and general evolution are still not well understood. Such an understanding, however, is important for several reasons. One is that seismogenic faults generate all the devastating earthquakes that occur on Earth. Another is that faults are major conduits of fluids, be it groundwater, geothermal water, gas, oil, or magma. The last term, magma, may surprise some, since the main conduits of magma are extension fractures, such as dykes, inclined sheets, and sills. However, many dykes use faults as parts of their paths, and many, perhaps most, transform faults are intruded by magma (e.g. Gudmundsson, 2007). Also, and most importantly in connection with hazards, the ring-faults of collapse calderas are commonly injected by magmas to form ring dykes.

Faults normally initiate from 'flaws' or weaknesses in the rocks. Such flaws include fossils, pores, microfractures, joints, contacts, and other stress raisers. In particular, in layered rocks, faults are often seen to initiate from sets of joints that were generated when the rock layers themselves were formed, such as cooling (columnar) joints, mud cracks (desiccation cracks), syneresis fractures (generated through dewatering and volume reduction of sediments), and cracks generated during mineral phase-change fractures, formed when volume is reduced as a result of mineral phase changes (for example during dolomitisation). In active areas, joints can commonly be seen to link up into faults, both in lateral and in vertical sections, during tectonic events (e.g., Gudmundsson, 2011; Larsen and Gudmundsson, 2010). The initiation of faults can thus be studied in the field, and also analysed in laboratory experiments on small samples (e.g., Lockner et al., 1991; Peng and Johnson, 1972), and is reasonably well understood.

The subsequent development and growth of the fault, once initiated, and its seismogenic activity are less well understood. Various geometric parameters have been studied, and their relations, in order to throw light on fault development and growth. These include (Fig. 1) fault length (strike dimension), fault width (dip dimension), total fault displacement, co-seismic slip in individual earthquake ruptures, and fault segmentation and segment linkage. One major conclusion is that the maximum (and mean) displacement on fault scales with the fault length or strike dimension (e.g., Clark and Cox, 1996; Schlische et al., 1996). Another conclusion is that the displacement–strike dimension ratios of faults differ widely from the co-seismic slip–rupture length

* Corresponding author. Tel.: +44 1784 276345.
E-mail addresses: a.gudmundsson@es.rhul.ac.uk (A. Gudmundsson), deguidi@unict.it (G. De Guidi).

0040-1951/$ – see front matter © 2013 Elsevier B.V. All rights reserved.
http://dx.doi.org/10.1016/j.tecto.2013.06.012

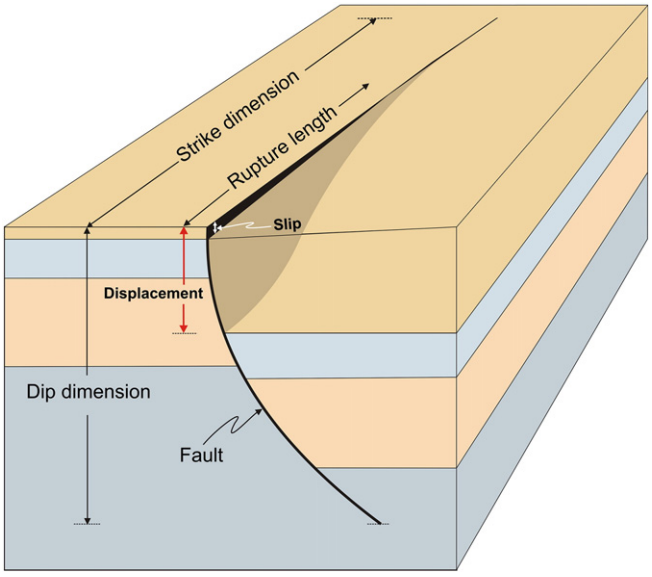

Fig. 1. Schematic illustration for the clarification of the terms strike dimension (fault-zone length), dip dimension (fault-zone width), displacement (total cumulative fault displacement), rupture length (co-seismic rupture length), and slip (co-seismic slip). The fault-zone example is a listric (curved) normal fault. The slip is regarded as recent and seen at the surface, whereas much of the cumulative displacement is buried (here we are supposed to see into the uppermost part of the crust, hence see the total cumulative displacement). Since the recent slip adds to the earlier displacement, the displacement does not refer to the same marker layer in the footwall as in the hanging wall. The layering is arbitrary except that the surface layer is much thicker in the hanging (right) wall of the fault than in its footwall. This difference is common in sedimentary basins and active volcanotectonic rift zones, where the surface sedimentary rocks or, for rift zones, the volcanic rocks, tend to accumulate and become much thicker in the hanging wall (or inside the graben in case the normal fault is a boundary fault of a graben). The scale is arbitrary — but to fit with the main data presented here the maximum displacement could be about 100 m and the maximum slip about 8 m. Only parts of the strike dimension and rupture lengths are shown (the vertical section cuts through the fault), and the rupture length is considerably shorter than the total length of the fault zone.

(strike dimension) ratios. In particular, the rupture length–slip ratios are commonly of the order of 10^{3-4} (Bonilla et al., 1984; Leonard, 2010; Wells and Coppersmith, 1994) whereas the fault length–displacement ratios are commonly of the order of 10^{1-2} (e.g., Clark and Cox, 1996; Schlische et al., 1996). These ratios thus differ by a factor that is normally of the order of 10^{1-2}.

Most of the studied and compared fault and earthquake rupture populations are from areas with widely different tectonic conditions and rock properties. Fracture-mechanics solutions (e.g. Broberg, 1999; Gudmundsson, 2011; Tada et al., 2000) indicate that the above ratios depend on the loading conditions and, in particular, on the mechanical properties of the rocks that the faults dissect. Since these properties vary widely between rocks of different origin and age, that are also commonly located within different tectonic regimes, it is difficult to isolate the parameters that primarily control the slip/displacement–length scaling relations and provide models to explain the relations.

Here we report results of a study of the slip/displacement–length scaling relations, both for faults and co-seismic ruptures, from a single comparatively small area, namely the eastern flank of the volcano Etna, Italy (Sicily). Almost all the studied faults and co-seismic ruptures dissect Holocene lava flows of essentially the same age and mechanical properties. We analyse 19 co-seismic ruptures and 7 faults and compare their geometric characteristics, including the scaling relations. For comparison, we also present fault data from the Holocene lava flows in the rift zone of Iceland. Using these data, together with data from the literature and analytical and numerical models, we provide a general growth model for faults. This model accounts for the difference in the slip/displacement–length scaling relations between co-seismic ruptures and faults and may also partly explain slow earthquakes and aseismic slip, features that are now known to be very common in active fault zones.

2. Definitions and previous studies

There have been many studies on the various aspects of the geometric and mechanical characteristics of faults and earthquake ruptures. In particular, there are many recent books and review papers on these topics (e.g., Jordan et al., 2003; Scholz, 2002; Turcotte et al., 2007; Yeats, 2012; Yeats et al., 1996) that provide detailed overview of the literature. The present summary of previous work is therefore brief.

Before summarising the main relevant previous results, however, a few definitions are in order. This follows because definitions of some of the parameters discussed, such as fault length, width, displacement, and slip, vary somewhat in the literature. In the present paper we use the following definitions (Fig. 1; cf. Gudmundsson, 2011):

- Fault is a planar discontinuity, a fracture, across which the main rock displacement is parallel with the fracture plane. A fault is thus primarily a shear fracture (modelled as a mode II or a mode III crack), while some (particularly normal) faults contain an opening (mode I) component and are thus mixed mode.
- Fault zone is a tabular rock body composed of two main hydromechanical units, a core and a damage zone. The core is mainly composed of breccias and gouge and the damage zone primarily of fractures of various types and trends. The words fault and fault zone are used interchangeably in this paper.
- Fault length is the strike dimension of the fault, as seen at the surface or as inferred for the subsurface from (usually geodetic and seismic) data.
- Fault width is the dip dimension of the fault as observed in the field (for very small faults) or as inferred from (usually geodetic and seismic) data.
- Fault displacement is the maximum (sometimes the mean) relative fracture-parallel movement of the fracture walls. Here displacement is always the total cumulative displacement; not the co-seismic slip in individual earthquakes.
- Co-seismic rupture length, or simply rupture length, refers to the strike dimension of the part of an active fault (or fault zone) that ruptures during a particular slip and an associated earthquake. Commonly, the rupture length is much shorter than the total length of the fault/fault zone within which the rupture (and earthquake) occurs.
- Co-seismic rupture width, or simply rupture width, refers to the dip dimension of the part of an active fault (or fault zone) that slipped during a particular co-seismic rupture and associated earthquake. For large faults/fault zones the width is the thickness of seismogenic layer (commonly 10–20 km). The rupture width of small to moderate earthquakes in large fault zones is normally much smaller than the total width of the fault/fault zone within which the rupture and earthquake occur.
- Co-seismic slip or simply slip is the displacement associated with the earthquake rupture. It is either measured at the surface, for a large earthquake, or inferred from the inversion of geodetic data, or both.
- Controlling dimension, as used in fault modelling, is the smaller dimension of the strike and dip dimensions.

There are many scaling relations for earthquakes. These include the Gutenberg–Richter frequency–magnitude relation, the Omori relation for the rate of aftershock production with time since the main shock, and the Bath's relation, indicating that the difference in magnitude between the main shock and the largest aftershock is nearly a constant. There are also other relations that are not as well established or accepted (e.g., Turcotte et al., 2007). These relate to the physics of earthquakes and the mechanics of rupture propagation.

Other types of scaling laws refer to the geometric aspects of the seismogenic faults and how they grow. As regards scaling relations between co-seismic lengths and slips, compilations of data include those by Ambraseys and Jackson (1998), Bonilla et al. (1984), De Guidi et al. (2012), Pavlides and Caputo (2004), and Wells and Coppersmith (1994). Other recent data on these scaling relations are presented by Biasi and Weldon (2006), Leonard (2010), Li et al. (2012), and Manighetti et al. (2009). Similarly, scaling relations between fault lengths and displacements have been compiled by many including Clark and Cox (1996), Cowie and Scholz (1992), Gudmundsson (2004), Li et al. (2012), Schlische et al. (1996), Shipton and Cowie (2001), Vermilye and Scholz (1998), and Walsh et al. (2002).

All these results show that the slip and displacements scale with the rupture/fault lengths. But they also show that there are no 'universal' scaling laws, neither for length versus displacements on faults nor for length versus slip on co-seismic ruptures. This is understandable because, as discussed in subsequent sections in the present paper, the scaling relations between length and slip/displacement depend on the fault geometry, the appropriate loading (and the type of loading, that is, mode II, mode III, or mixed mode) and, in particular, the mechanical properties of the host rock (primarily Young's modulus). Since all these factors, particularly the mechanical properties, vary between different areas and between individual faults, it would have been surprising to find any sort of universal scaling laws.

Perhaps the most striking result of these studies is the great difference between the rupture length–slip ratios and the fault length–displacement ratios. As indicated above, the rupture length–slip ratios are commonly of the order of 10^{3-4} (e.g., Bonilla et al., 1984; Leonard, 2010; Wells and Coppersmith, 1994). By contrast, the fault length–displacement ratios are commonly of the order of 10^{1-2} (e.g., Clark and Cox, 1996; Schlische et al., 1996). These scaling relations thus differ by factors that are commonly of the order of 10^{1-2} and may, occasionally, be of the order of 10^3.

While these differences in scaling relations between rupture length–slip and fault length–displacement have been known for some time, little attempt has been made to explain them. Walsh et al. (2002) suggested that most active faults reach their total lengths rapidly and subsequent slips on the faults simply accumulate while the fault length does not increase. The main idea of Walsh et al. (2002) is that the fault lengths are 'inherited from the underlying structure and established rapidly' and that the near-constant length of the fault during most of its active lifetime is due to 'retardation of lateral propagation by interaction between fault tips'. Since faults grow through segment interaction and linkage, and since theoretically the maximum stress concentration normally occurs at the tip of a loaded fracture (e.g., Broberg, 1999), it is perhaps not entirely clear in this conceptual model under what mechanical conditions the lateral propagation and/or linkage would become retarded or arrested.

Another attempt to explain this difference is through consideration of the variation in the mechanical properties of the fault zones that, to a large degree, determine fault displacement and co-seismic slip (Gudmundsson, 2004). Here the main ideas are, first, that Young's modulus or the stiffness of a fault zone changes during its evolution; in particular, that the stiffness of the core and the damage zone normally decreases with time for an active fault. Secondly, that the dynamic Young's modulus controls the rupture length–slip ratio, whereas the static Young's modulus controls the fault length–displacement ratio. Both ideas suggest that the rupture length–slip ratio may be one to three orders of magnitude larger than the fault length–displacement ratio. Gudmundsson (2004), however, does not discuss (1) how the fault zone grows so as to reach the measured length–displacement ratios, (2) the contribution of aseismic slip and slow earthquakes to the overall fault displacement and the differences in the above ratios, and (3) why the lateral tips stop propagating (become arrested) so that the fault is able to maintain an essentially constant strike dimension through much of its history. In the present paper, we consider these three points and show how they, and other factors related to fault growth, contribute to explaining the difference in the rupture length–slip and fault length–displacement ratios.

3. Power laws: earthquake magnitudes and fracture lengths

To understand the fault length–displacement and the rupture length–slip distributions, we must first have an overview of the length–size distribution of faults and other rock fractures that occur in fault zones. Measurements worldwide show that the length–size distributions of rock fractures in general, and those of faults in particular, commonly follow power-law (heavy-tailed) distributions (e.g., Gudmundsson and Mohajeri, 2013; Mohajeri and Gudmundsson, 2012; Turcotte, 1997). An example of the length–size distribution of fractures in the Holocene rift zone of Iceland (Fig. 2) shows that the consequence of the negative slope is that there are many short fractures and comparatively few long fractures. These results indicate that the length–size distributions of faults within fault zones scale in similar ways as the magnitudes of the earthquakes within these zones, which are known to follow power laws.

More specifically, the earthquake size or magnitude distributions in any area, any active fault zone, follow power laws, namely in the form (e.g., Kasahara, 1981):

$$N(\geq M) = 10^{a-bM} \tag{1}$$

which, in seismology, is more commonly written in the form:

$$\log N(\geq M) = a - bM \tag{2}$$

where N is the number of earthquakes with a magnitude larger than M, and a and b are constants. Constant b is commonly referred to as the b-value; its value varies between different active areas and between different individual fault zones. The b-value is mostly in the range $0.8 < b < 1.2$ (e.g. Turcotte et al., 2007) and is commonly taken as 1.0. Changes in the b-value are often regarded as precursors to large earthquakes (Smith, 1981) and, for volcanic areas, precursors to eruptions (Gresta and Patanè, 1983a,b).

Similar to the size distribution of earthquake magnitudes, there is commonly a power-law size distribution of the lengths of faults in seismically active areas in the form:

$$P(\geq x) = cx^{-\gamma}. \tag{3}$$

Here, $P(\geq x)$ refers to the number or frequency of fractures with a length larger than x. In Eq. (3), c is a constant of proportionality and γ is the scaling exponent. As is the case for earthquake magnitudes, the power law for fracture lengths can also be presented by taking the logarithms on both sides of Eq. (3), in which case the equation becomes:

$$\log P(\geq x) = \log c - \gamma \log x. \tag{4}$$

Eqs. (2) and (4) clearly represent a straight line. Indeed, a common procedure to test if a probability distribution is really a power law is to log-transform the data, that is, to plot them on a bi-logarithmic (log–log) plot. If the resulting curve is a straight line, then that is regarded as a general indication that the data follow a power law. The slope of the straight line is the scaling exponent γ. Because the number of objects (here fractures) normally increases as they become smaller (shorter), the slope is negative. The scaling exponent, however, is defined as the negative of the slope and is thus a positive number. To find out if a power law best describes the dataset, or if some other functions give a better fit, several different types of tests can be used (Clauset et al., 2009; Mohajeri and Gudmundsson, 2012). When the data are plotted using bins of given widths or class limits, then all fractures in a given bin exceed the length x. If the bin width (class limits) of

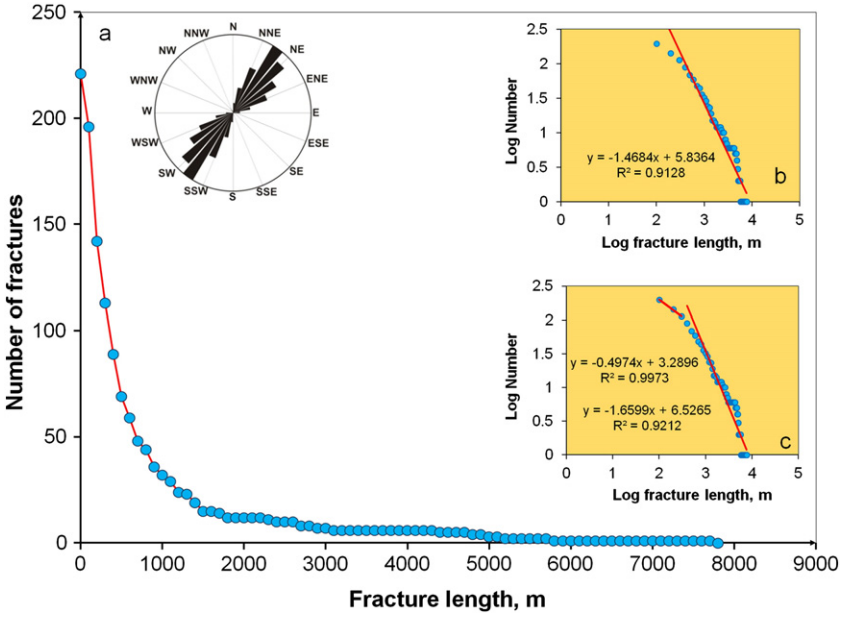

Fig. 2. Example of length-size distributions of tectonic fractures, here cumulative distribution of 221 tension fractures and normal faults, in the Holocene lava flows of the rift zone in Southwest Iceland. Inspection of the curve indicates a power-size length distribution. When the fracture lengths are plotted as a log–log (bi-logarithmic) plot the data are seen to be with a break, so that a double power law fits the distribution better than a single power law. The different slopes on the bi-logarithmic plot represent the different scaling exponents (Eq. (3)). (a) A cumulative power-law distribution for fracture lengths, and a rose diagram for fracture strike (inset). Total number of tectonic fractures, N, is 221 and their lengths range from 40 m to 7736 m. (b) A bi-logarithmic plot of the fractures showing the break in the straight-line slope. The estimated coefficients of determination (R^2) are indicated (cf. Gudmundsson and Mohajeri, 2013; Mohajeri and Gudmundsson, 2012).

200 m is used, for instance, then all fractures longer than 0 m fall into the first bin, all fractures longer than 200 m fall into the second bin, all fractures longer than 400 m fall into the third bin, and so on.

The slip/displacement size distributions on faults also commonly follow power laws (Fig. 3). This is understandable since, for elastic crack models, there is a linear relation between the controlling dimension – the shorter of the strike and dip dimensions (Gudmundsson, 2011) – and the slip/displacement. Thus, since the length distribution follows a power law, one could expect the slip/displacement distribution to do likewise (Fig. 3). For example, for simple through-crack mode III model of a seismogenic fault, the relationship between fault displacement Δu and the controlling dimension of the fault is given by Broberg (1999), Gudmundsson (2011), and Tada et al. (2000) as:

$$\Delta u_{III} = \frac{2\tau_d(1+\nu)L}{E} \tag{5}$$

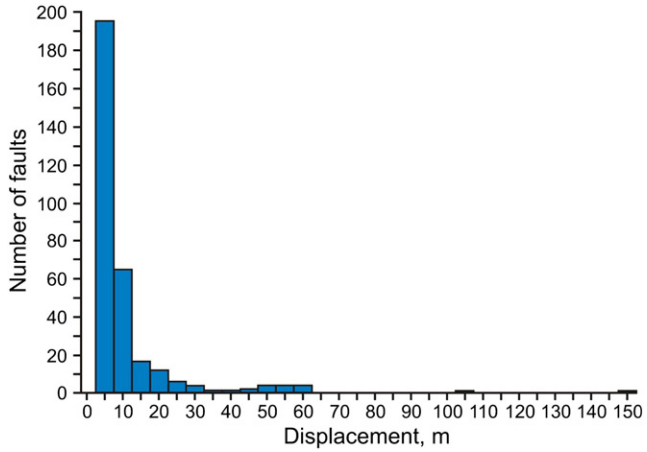

Fig. 3. Displacement–size distribution of 315 normal faults in Iceland. The distribution follows approximately a power law (Forslund and Gudmundsson, 1992).

for the case where the length or strike dimension (Fig. 1) L is the controlling dimension of the fault, and as:

$$\Delta u_{III} = \frac{4\tau_d(1+\nu)R}{E} \tag{6}$$

for the case where the dip dimension R is the controlling dimension of the fault. In Eqs. (5) and (6), ν is Poisson's ratio, E is Young's modulus, and τ_d is the driving shear stress (roughly equal to the earthquake stress drop).

More specifically, the driving shear stress is defined as the difference between the shear stress τ on the fault plane and the residual frictional or shear strength τ_f on the plane after fault slip (Gudmundsson, 2011; Nur, 1974), namely as:

$$\tau_d = \tau - \tau_f. \tag{7}$$

The residual frictional strength is commonly interpreted as being equal to the third term in the Modified Griffith criterion, which is a development of the well-known Coulomb criterion and given by (Gudmundsson, 2011; Nur, 1974):

$$\tau_d = 2T_0 + \mu(\sigma_n - p_t) \tag{8}$$

where T_0 is the in-situ tensile strength of the fault rock, μ is the coefficient of internal friction, σ_n is the normal stress on the fault plane, and p_t is the total fluid pressure acting on the fault plane at the time of fault slip. It is well known that all tectonic earthquakes occur under high fluid pressure. When the fluid pressure approaches or reaches the normal stress σ_n on the fault plane, the term $\mu(\sigma_n - p_t)$ becomes close to or reaches zero. As said, a common interpretation of the frictional strength is that $\tau_f = \mu(\sigma_n - p_t)$. It follows that, under high fluid pressure, the frictional strength may be close to or actually zero.

Occasionally, the fluid pressure on the fault plane may be so high as to make the term $\mu(\sigma_n - p_t)$ negative, which is presumably one reason why the driving stresses, as inferred from stress drops, for many earthquakes are a fraction of a mega-Pascal. Generally, the high fluid pressure on a fault plane reduces the friction and the normal stress (commonly to

zero) so as to make fault slip possible at low driving shear stresses down to depths of tens or hundreds of kilometres (such as in subduction zones).

For large strike-slip faults, R is the width or dip dimension of the fault (Fig. 1), and Eq. (6) is used. A mode II model might be used, however, if the strike-slip fault dissects a crustal segment with a free surface at the fault top and bottom, such as would be the case if the fault were located in the crustal segment above a fluid magma body (Gudmundsson, 2011). Most through-going dip-slip faults are modelled using Eq. (5), in which case L is the strike dimension (surface length) of the fault (Fig. 1).

The moment or energy M_0 associated with an earthquake is given by:

$$M_0 = \Delta u A G \tag{9}$$

where, as before, Δu is the (average) slip, A is the area of the co-seismic rupture, and G is shear modulus or the modulus of rigidity. M_0 has the units of energy, that is, Nm in SI units. In earthquake mechanics, however, dyne-cm is still commonly used. It follows from Eq. (9) that the energy released in an earthquake scales with the area of the co-seismic rupture, and thus with the dimensions of the rupture plane. The moment is also directly proportional to the co-seismic slip Δu. Thus, the correlations between the dimensions (e.g., the rupture length) and the slips are of fundamental importance for understanding the energy released during a seismogenic faulting.

Magnitude scales reflect the energy released during an earthquake. In particular, the moment magnitude scale relates to the moment, that is, the energy released, as given by Eq. (9). Since the moment is directly proportional to the areas and slips of the co-seismic ruptures, both of which have power-law size distributions, it follows that earthquake size or magnitude distributions must follow power laws, as indeed they do (Eqs. (1), (2)). Thus, the power-law earthquake-magnitude size distributions are a direct consequence of the fact that in seismically active areas (and in individual fault zones) the size distributions of the earthquake-producing faults themselves follow power laws.

4. Length–slip/displacement distributions

We studied 7 faults and 19 co-seismic ruptures in the eastern flanks of the volcano Etna in Italy (Figs. 4, 5). The unique aspect of the present data is, first, that most of the co-seismic length–slip data and the length–displacement data are from the same faults (Fig. 5). In Fig. 5, the full dots indicate cumulative total displacements, whereas the empty dots represent co-seismic slips. Secondly, nearly all the faults dissect the same Holocene lava flows on the east flanks of Etna (Fig. 4) so that the mechanical properties of the rocks hosting the faults are generally very similar.

Consider first the length–displacement ratios of the 7 faults (Fig. 5). All the faults except one are primarily dip slip or, more specifically, normal faults. The one exception is a sinistral strike-slip fault. In addition, one of the normal faults has a dextral component. The lengths or strike dimensions of these faults range from 1150 m to 12,950 m, with an average length of about 6341 m. The maximum displacements on the faults range from 8 m to 190 m, with an average maximum displacement of about 73 m.

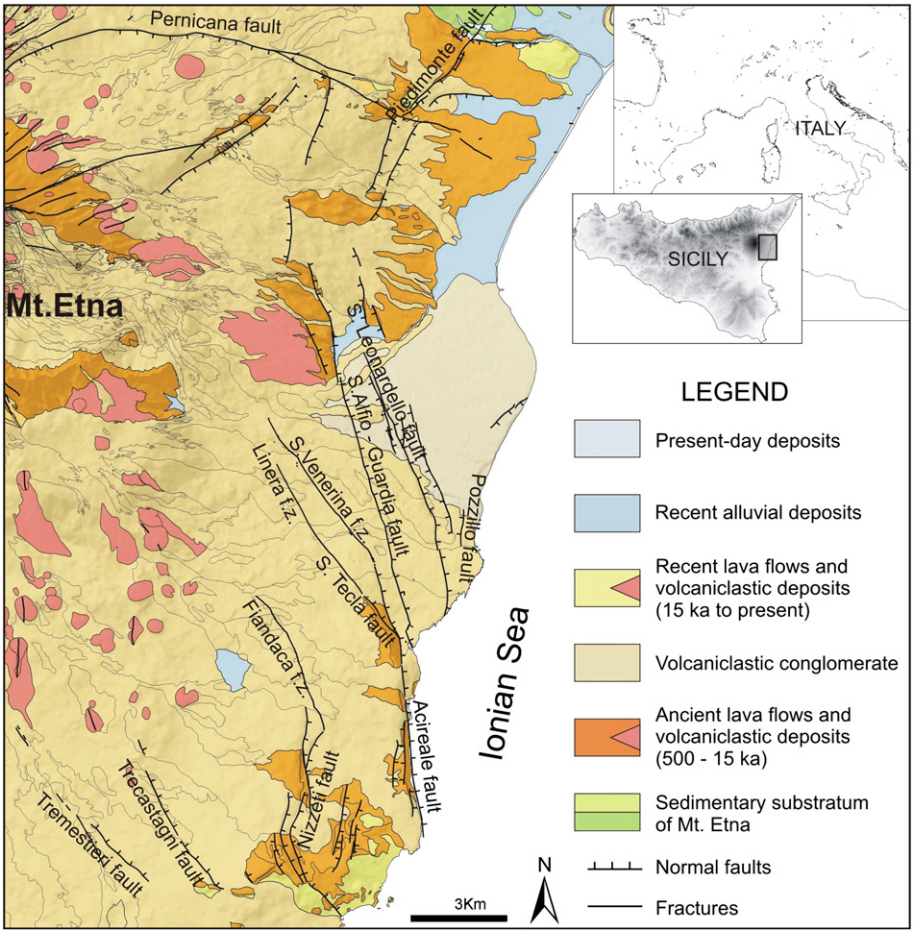

Fig. 4. Geological map of the eastern flank of Mt. Etna and location of the faults studied. Modified from Monaco et al. (2008).

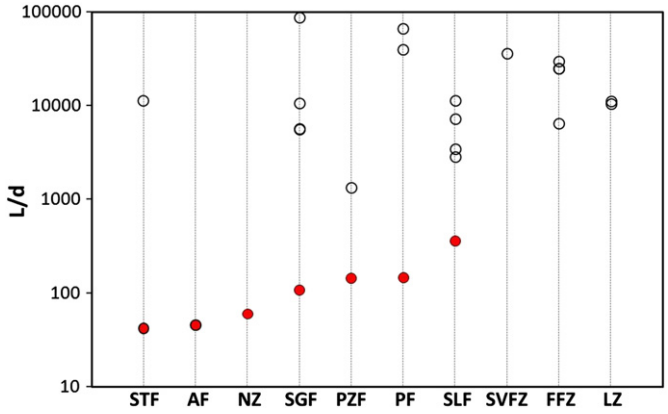

Fig. 5. Displacements/slips on faults and seismogenic ruptures ordered according to a possible progressive relative age of activity. Empty and full dots indicate coseismic and cumulative displacements, respectively. Abbreviations: STF: Santa Tecla fault; AF: Acireale fault; NF: Nizzeti fault; SGF: S.Alfio-Guardia fault; PF: Pozzillo fault; PF: Pernicana fault; SLF: San Leonardello fault; SVFZ: Santa Venerina fracture zone; FFZ: Fiandaca zone. For location see Fig. 4.

The length–displacement ratios range from 42 to 362, with an average value of about 130. Thus, the largest length–displacement ratio is about 8.6-times larger than the smallest one. The two smallest length–displacement ratios, 42 and 46, belong to the normal fault with the dextral component (and thus a mixed-mode fault) and to the sinistral strike-slip fault. All the other ratios are obtained from essentially pure normal faults.

The co-seismic ruptures belong to 5 of the faults discussed above, as well as to 3 additional diffuse fracture zones. These 3 fracture zones have no cumulative fault displacements at the surface and are thus distinguished from the faults (all of which have cumulative surface displacements, as indicated above). Two of the faults have not been subject to recent earthquakes and are therefore not shown with co-seismic length–slip ratios (Fig. 5). The co-seismic ruptures range in length from 100 m to 6500 m, with an average rupture length of 3657 m. The co-seismic slips range from 0.03 m (3 cm) to 1.08 m, with an average slip of about 0.31 m (31 cm).

The co-seismic length–slip ratios range from 1333 to 87,500, with an average length–slip ratio of 19,595. This means that the largest length–slip ratio is about 66-times larger than the smallest ratio. Also, the average length–slip ratio is about 150-times larger than the average length–displacement ratio. Thus, they differ by about two orders of magnitude.

Clearly, the maximum length and the average length of the co-seismic ruptures are much smaller than those of the associated faults. This is understandable since, normally, only a part of a fault or a fault zone ruptures during an earthquake (Fig. 1); the entire fault zone ruptures the largest earthquakes that the fault zone is capable of generating. The power-law size distribution of earthquake magnitudes (Eqs. (1), (2)) applies also to individual fault zones, as does the power-law size distribution of the fractures and faults within that fault zone (Eqs. (3), (4)). Similarly, the maximum co-seismic slip and the average slip are much smaller than the maximum displacement and the average displacement on the faults.

5. Fault growth

Faults, like other rock fractures, grow by the accumulation of displacement or slip events. Eqs. (5) and (6) show that, for constant Young's modulus E and Poisson's ratio ν, the ratio between the controlling dimension of the fault, that is, either the strike dimension or the dip dimension (L or R), and its displacement/slip should be constant so long as the driving stress (here τ_d) is constant. These results apply to through-the-thickness or through-crack models, as given by Eqs. (5) and (6). However, a part-through crack model yields essentially the same results.

Consider, for example, a dip-slip fault where the dip dimension R controls the displacement. Most of the faults considered here are dip-slip faults, and for the small slips observed during most of the co-seismic ruptures, the fault is unlikely to have penetrated the entire seismogenic layer, and should therefore be modelled as mode II part-through crack. For such a crack model, the displacement Δu_{II} is related to the dip dimension R of the fault through the equation (Tada et al., 2000; cf. Gudmundsson, 2011):

$$\Delta u_{II} = \frac{4\tau_d RV}{E} \tag{10}$$

where the function V is given (using radians) by:

$$V = \frac{1.46 + 3.42\left[1 - \cos\left(\frac{\pi R}{2T}\right)\right]}{\left[\cos\left(\frac{\pi R}{2T}\right)\right]^2} \tag{11}$$

where T is the total thickness of the elastic crustal segment hosting the fault zone. For most major fault zones, T would be roughly equal to the thickness of the seismogenic layer (commonly 10–20 km). Again, in Eq. (10) we see that there is a linear correlation between length and slip/displacement. Thus, for elastic crack models, there should be a linear correlation between the slip/displacement on a fault and the size of its controlling dimension.

Whether the correlation between the controlling dimension, particularly the strike dimension, and slip/displacement on faults is actually linear or nonlinear has been the matter of discussion for many years (e.g. Cowie and Scholz, 1992; Gillespie et al., 1992; Leonard, 2010; Schlische et al., 1996). There have also been many studies on the relation between the earthquake energy release or moment (Eq. (9)) and the controlling dimensions (strike or dip) of the co-seismic rupture planes (e.g., Kagan, 2002; Romanowicz and Ruff, 2002). Many of these works have focused primarily on the relationship or scaling with the rupture length (strike dimension). However, so long as the slip/displacement is in accordance with elastic fracture-mechanics models (Eqs. (5), (6), (10)), it should be the smaller of the strike and dip dimensions, the controlling dimension (Gudmundsson, 2000), that has the greater effect on the fault displacement.

Studies indicate that some faults are close to circular in geometry, in which case the strike and dip dimensions are equal in size so that either can be regarded as the controlling dimension (e.g., De Guidi et al., 2012; Nicol et al., 1996). For other (but fewer) faults the controlling (smaller) dimension is the strike dimension, while for many faults the dip dimension is the smaller and thus the controlling dimension. The length–slip/displacement scaling would show the correct relation for circular and strike-dimension controlled faults, but rather less so for the common dip-dimension controlled faults.

While faults grow through the accumulation of slip, the relation between the accumulated slip and the fault expansion (increase in strike and dip dimensions) remains unclear. When all the faults are young and dissect the same rock unit, there is sometimes a good correlation between the strike dimension and the fault displacement (Gudmundsson, 2000, 2005). For example, Holocene normal faults in Iceland show a strong linear correlation between the maximum vertical displacement and the strike dimension (Fig. 6). There are also linear correlations between the lengths of the co-seismic ruptures and their slips, as well as between the lengths of the faults and their displacements for the Etna faults. The linear correlations are significant for the Etna faults and co-seismic ruptures (Fig. 5), although somewhat weaker (the linear correlation coefficient $r = 0.6$ for both the ruptures and the faults) than for the Holocene faults in Iceland.

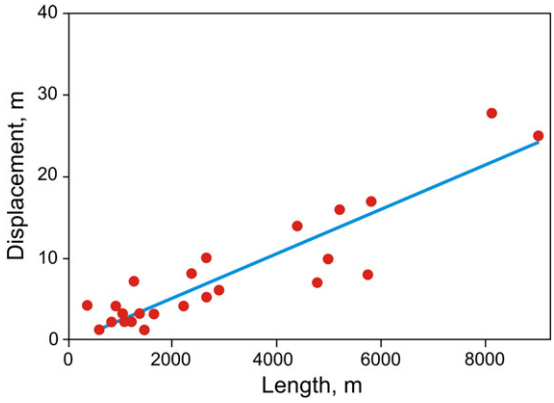

Fig. 6. Linear correlation between Holocene displacement and length (strike dimension) of 26 normal faults from the rift zone of Iceland (Gudmundsson, 2000).

Faults grow partly through the accumulation of seismic slip events, and partly through accumulation of aseismic slip events. The seismic slip events, such as in Fig. 5, are well documented and we shall first look at these. It is clear from the data presented here (Fig. 5) that the seismic slip in a particular fault zone is not related to the accumulated or cumulative slip in that fault zone at the time of the earthquake. Thus, the co-seismic length–slip ratios do not correlate with the existing length–displacement ratios. For example, fault SGF with a length–displacement ratio of 108 has co-seismic length–slip ratios from 5560 to 87,500, whereas fault SLF with a length–displacement ratio of 362 has co-seismic length–slip ratios from 3472 to 11,429, a much smaller range and a much smaller maximum.

Part of the growth of a fault is through aseismic slip (sometimes referred to as creep). Aseismic slip is very common on faults (e.g., Galehouse and Lienkaemper, 2003; Jordan et al., 2003; McFarland et al., 2009; Peng and Gomberg, 2010; Rolandone et al., 2008; Sleep and Blanpied, 1992). In this context, part of the aseismic slip may be referred to as afterslip, the slip following the main seismic event. Afterslip is normally partly seismic and partly aseismic.

Given this information, we now propose to explain the difference between the co-seismic length–slip ratios and the length–displacement ratios on fault zones (Fig. 5). If we take Eqs. (5) and (6) as the basic fracture-mechanics models for through faults (for part-through faults the basic models would be Eqs. (10), (11)), then there are clearly four factors that could affect the differences in these ratios: namely, the driving shear stress (τ_d), the size of the controlling dimension (R or L), Poisson's ratio (ν), and Young's modulus (E).

The driving shear stress corresponds roughly to the stress drop associated with a seismogenic slip and is commonly in the range of 0.1–10 MPa, the overall general range being around 0.03–30 MPa (Kanamori and Anderson, 1975; Scholz, 2002). The stress drops for 175 earthquakes in Etna are shown in Fig. 7. For the Etna earthquakes, the stress drops range from about 0.1 MPa to about 10 MPa, with most values between 0.5 MPa and about 5 MPa. As is observed in other active areas, the stress drop does not show any clear relationship with the earthquake magnitudes, which range mostly from about M1 to M4. The difference between the co-seismic length–slip ratios and the length–displacement ratios are thus unlikely to be primarily related to differences in driving shear stress or stress drop.

The size of the controlling dimension clearly affects the slip/displacement for given driving stresses and mechanical properties (Eqs. (5), (6)). However, many and perhaps most faults reach their final strike dimension comparatively rapidly and do not propagate laterally beyond that length. This is well known from active rift zones, such as in Iceland, where many large Holocene normal faults have reached lengths that do not change during rifting episodes (e.g. Gudmundsson, 2005), and similar observations have been made of faults elsewhere (Walsh et al., 2002). The dip dimension, however, is likely to increase in size until it reaches the thickness of the seismogenic layer, which is commonly 10–20 km in continental areas.

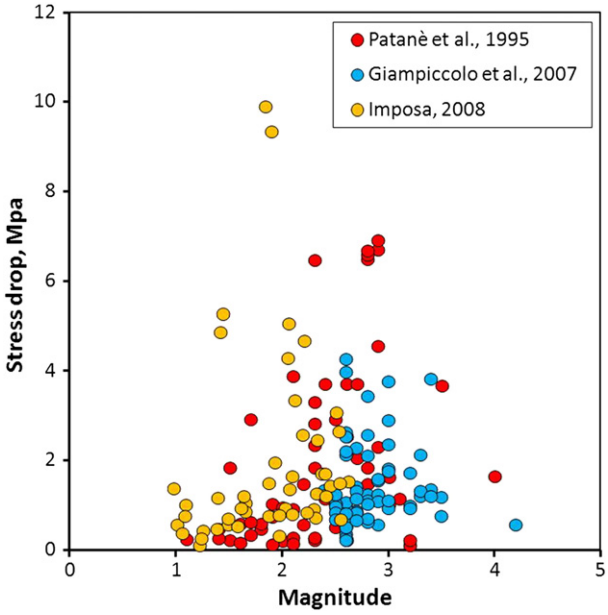

Fig. 7. Compilation of stress drops versus magnitude for 175 earthquakes in Etna. Data are from Giampiccolo et al. (2007), Imposa (2008), and Patanè et al. (1995).

Poisson's ratio is similar for rocks of various types, generally between 0.15 and 0.30, the most common value being around 0.25 (Gudmundsson, 2011). There is thus little reason to expect variations in Poisson's ratio to be a significant contribution the difference between ratios of length–slip of seismogenic ruptures and ratios of length–displacement of existing faults.

In contrast to the small variation in Poisson's ratio, Young's modulus, E, varies widely inside fault zones and between rock layers and units in general. Young's modulus is a measure of stiffness, that is, how much force/stress on a material body is needed for a given displacement/strain. It follows that soft or, more correctly, compliant materials such as many sedimentary rocks and highly fractured rocks have a relatively low Young's modulus, whereas stiff rocks, such as many dense and non-fractured igneous and metamorphic rocks, have a comparatively high Young's modulus.

There are some general statements that may be made about Young's modulus and its measurements, namely the following:

(1) The dynamic modulus for a given rock body or specimen is normally greater than the static modulus, the difference being as much as 13-times (Goodman, 1989). The greatest difference is normally at low confining pressure, that is, at shallow crustal depths. The static modulus is suitable for modelling processes that are slow in comparison with the velocities of propagation of seismic waves, that is, much slower than kilometres per second. By contrast, the dynamic modulus is suitable for modelling co-seismic ruptures.

(2) Laboratory measurements on small samples, dynamic or static, are commonly 1.5 to 5-times greater than the in-situ or field modulus of the same type of rock (Heuze, 1980). More specifically, the laboratory modulus of rocks is commonly 3-times the field modulus (Fjaer, 2009; Gudmundsson, 2011; Heuze, 1980; Ledbetter, 1993).

(3) When the mean stress increases, that is, at greater crustal depths, Young's modulus also generally increases (Heuze, 1980). By contrast, increasing temperature, porosity and water content all decrease Young's modulus.

(4) At shallow crustal depths, particularly in tectonically active areas, the most important effect on the magnitude of the field Young's modulus is the number of fractures per unit volume of the rock mass (e.g., Priest, 1993). Young's modulus of a rock mass is normally less than that of laboratory sample of the same type of rock. This difference is mainly attributed to fractures and pores in the rock mass, which do not occur in the small laboratory samples.

(5) The ratio E_{is}/E_{la} (E in situ/E laboratory) shows an exponential or a power-law decay as the frequency of fractures increases. Because of this, it is also clear that the effects of increasing fracture frequency is greatest in the beginning, that is, in the range of 2–10 fractures per metre. Thus fracturing normally decreases Young's modulus.

Fault zones consist of two main hydromechanical units: a core and a damage zone (Fig. 8; e.g., Bruhn et al., 1994; Caine et al., 1995; Gudmundsson et al., 2010). The core takes up most of the fault displacement and contains many faults and fractures, though normally much smaller than in the fault damage zone. The characteristic features of the core, however, are breccias, gouge, and other cataclastic rocks. In active fault zones, the core rock is commonly crushed and altered into a soft material that can fail as brittle only during the high strain rates associated with seismogenic faulting. As the core develops, its cavities and fractures may become gradually filled with secondary minerals, thereby making the core stiffer. However, during fault slip the core has a granular-media structure at the millimetre or centimetre scale. In major fault zones, the core thicknesses may reach from several metres to tens of metres.

The damage zone contains breccias but is primarily composed of sets of fractures that normally increase (regularly or irregularly) in frequency on approaching the fault core. It follows that in the damage zone the effective Young's modulus, which depends strongly on the fracture frequency (Priest, 1993), tends to decrease towards the core. In an active fault zone, the fault gouge and breccia of the core itself would also normally have a low Young's modulus, commonly similar to that of clay, weak sedimentary rocks, or pyroclastic rocks such as tuff (Bell, 2000; Gudmundsson, 2011; Heap et al., 2009; Hoek, 2000).

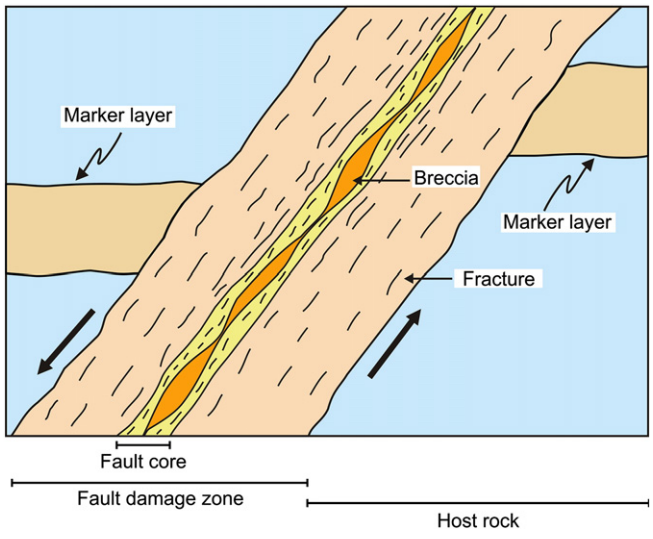

Fig. 8. Schematic illustration of a fault core and fault damage zone in a normal fault. The core is mainly composed of breccia and gouge whereas the damage zone is characterised by fractures that vary in frequency (the frequency generally decreases) with increasing distance from the core. The thickness of the breccia/gouge normally varies along the fault plane.
Modified from Gudmundsson (2005).

As the fault displacement increases so does the thickness of the fault zone; both the thickness of the core (Fig. 9) and the thickness of the damage zone (Gudmundsson et al., 2010). More specifically, as the fault zone grows there will be gradually thicker zones of brecciated and fractured fault rocks within the fault zone. Because the fault rocks constituting the damage zone and the core are normally soft in comparison with the host rocks, it follows that the stiffness of an active fault zone decreases with time.

6. Explanation of the length–slip/displacement ratios

One remarkable observation is that the length–slip and length–displacement ratios on the same fault are commonly widely different (Fig. 5). More specifically, the co-seismic rupture has normally a completely different length–slip ratio from the general length–displacement ratio of the fault zone within which the earthquake occurs. Since the equations controlling both ratios are the same, namely Eqs. (5), (6), and (10) or, depending on the exact fault geometry, other similar fracture-mechanics equations (e.g. Tada et al., 2000), it follows that somehow the mechanical properties that control the different aspect (length–slip/displacement) ratios must be different.

We have concluded above that the most likely property to vary during the evolution of a fault zone is its effective stiffness or Young's modulus. The first difference among effective stiffnesses relates to the dynamic and static Young's moduli. We have suggested that during an earthquake rupture, it is the dynamic Young's modulus that controls the co-seismic length–slip ratio. By contrast, the long-term length–displacement on the same fault is controlled by the static Young's modulus. As we have seen above, these moduli can, particularly at shallow depths (where most co-seismic ruptures are measured), easily differ by an order of magnitude.

The difference between static and dynamic Young's moduli, however, can be even greater. In active fault zones the inner part of the damage zone and the core itself may be very compliant (soft) (Fig. 8). It is this very soft core and the innermost part of the damage zone that determine the long-term length–displacement ratio. For soft breccias and gouge in the core, and highly fractured innermost parts of damage zone, the static Young's modulus may be 0.1 GPa or less (Gudmundsson, 2011), whereas the dynamic modulus controlling the co-seismic length–slip ratio may reflect and be controlled by the dynamic Young's modulus in other parts of the fault zone, such as the inner or outer damage zone, and be one or two orders of magnitude higher.

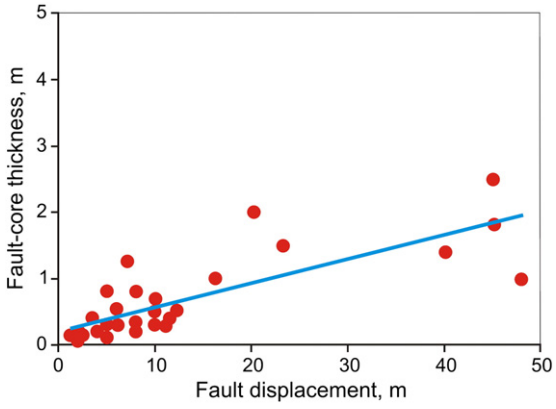

Fig. 9. Variation in the thickness of fault core as a function of vertical displacement on 28 Pleistocene and late Tertiary normal faults in Iceland. The linear correlation coefficient $r = 0.78$. However, a non-linear curve might fit the data better, and suggests that the rate of fault–core thickness increase slows down as the fault displacement increases (Forslund and Gudmundsson, 1992).

The basic conceptual model proposed here is as follows. Following a co-seismic slip controlled by the dynamic Young's modulus of the ruptured part of the fault zone, the final displacement adjusts to the long-term or static Young's modulus in the core and the innermost part of the damage zone. This adjustment is largely through aseismic slow-slip processes (cf. Peng and Gomberg, 2010). Some adjustment may be through aftershocks, but those would be controlled by the dynamic Young's modulus, so that the aspect ratio of length to slip would remain basically the same. In the present model, the main adjustment is through aseismic (slow) slip (including afterslip) and the associated general 'creep'.

There are many terms in current use that may, depending on how they are interpreted, refer to aseismic slip. One of these is 'slow earthquake', another is creep in the uppermost part of the fault zone, and the third one is 'slow-slip pheomena' (Galehouse and Lienkaemper, 2003; Jordan et al., 2003; McFarland et al., 2009; Peng and Gomberg, 2010; Rolandone et al., 2008; Sleep and Blanpied, 1992). Part of the aseismic slip occurs through 'afterslip' and part through 'creep', but here we refer to all these aseismic slip processes simply as aseismic slip. Aseismic slip is very common. It is estimated that in subduction and transform zones, around 50% of the slip is aseismic (Stein and Wysession, 2003; cf. Peng and Gomberg, 2010).

In the model proposed here, aseismic slip is a partly the result of a 'correction' or adjustment of the slip to that which would have occurred if the dynamic Young's modulus controlling the co-seismic slip was equal to the static modulus of the core and the innermost part of the damage zone. In this sense, the model is analogous to an elastic–plastic model where to the initial elastic strain or displacement there is gradually added viscous strain. The latter, in this case, is the aseismic slip for adjustment to the long-term static Young's modulus. Similar models may be based on the theory of viscoelasticity rather than elastic–plastic models. Thus, following each co-seismic slip there will be an aseismic slip on the fault that is controlled by the static modulus of its core and innermost damage zone that gradually brings the original length–slip ratio closer to the general length–displacement ratio.

In some ways, there is hardly any limit to the cumulative displacement that can occur on a fault. The analogy with dyke injections is clear. In a swarm of dykes, the dilation or opening may range, in traverses or profiles of kilometres or more, from less than 1% to 100% (Gudmundsson, 2011, 2012). The ophiolites and swarms of inclined (cone) sheets commonly reach 80–100% dilation, indicating that almost the entire rock is composed of dykes/sheets. Since the swarms are of limited extent – usually several kilometres for cone sheets and tens or hundreds of kilometres for dyke swarms – it is clear that a single swarm can have a very low length/opening displacement (cumulative thickness) ratio, just like faults.

The question remains, however, as to why faults stop propagating laterally while accumulating increasing displacement. The main reasons must be, first, the unfavourable changes in the local stress field at the tips, favouring arrest of the lateral propagation of the fault and, second, that the limited energy available for the fault propagation is used for increasing its displacement rather than length (cf. Gudmundsson, 2012). As the damage zone and core of a fault evolve, it becomes gradually easier for the fault to slip within the existing core/damage zone rather than to develop new segments or extensions at one or both its lateral ends. Many faults dissipate their energy through creep; others dissipate their strain energy most easily in the core and damage zone rather than through lateral extensions into new and largely non-fractured host rocks.

No transverse faults or other discontinuities are needed to limit the lateral growth of a fault. In fact, the common power-law size distributions of fault lengths, and fracture lengths in general, show that most fractures stop their propagation after reaching a comparatively short length (Fig. 2). More specifically, in any rift-zone segment with many faults, most of the faults remain short, and with small displacements, in comparison with the longest fault (Figs. 2, 6). After this comparatively short length is reached, the fault may still continue to grow and change its geometry thorough accumulation of slip resulting in a gradually increasing displacement and a decreasing length–displacement ratio (Fig. 5).

7. Discussion

The essential function of faults is to accumulate displacement or strain; in other words, to allow the brittle or quasi-brittle crust to deform. Most earthquakes and slips occur on existing faults (Fig. 10); the formation of new faults is much less frequent than the slip on old faults. It is well known that even if the local stress field changes so that an existing fault is no longer optimally orientated in relation to the principal stresses, slips and earthquakes tend continue on the fault long after it becomes unfavourably oriented (e.g., Faulkner et al., 2006; Sibson, 1990). This is partly because faults are weak – tolerate less shear stresses before failure or slip than the surrounding 'intact' host rock – and partly because faults tend to concentrate stresses, that is, they are stress raisers.

Most active fault zones are mechanically weak in the sense that they tolerate less shear stress before slip than their surroundings (e.g., Hickman et al., 2007; Zoback, 1991; Zoback et al., 2011). One obvious reason for the weakness is that a typical fault damage zone and core is composed of weak rocks; in particular the core contains soft breccias, clays, and, in the San Andreas fault, talc. Stress measurements indicate that close to active faults, such as San Andreas, the differential stress is comparatively low, in agreement with the faults being weak (Zoback et al., 2011). Because the fault damage zone and core are composed of rocks with mechanical properties that are normally widely different from those of the host rock, fault zones concentrate stresses, both in the damage zone and the core and at the contacts between the damage zone and the host rocks (e.g., Gudmundsson et al., 2010). This follows because a fault zone acts as an elastic inclusion or inhomogeneity that, because its mechanical properties are different from those of the host rock, concentrates stresses and modifies the local stress field (e.g., Eshelby, 1957; Gudmundsson, 2011; Savin, 1961).

These considerations indicate that, once formed, a fault zone tends to be reactivated even if it is unfavourably oriented in relation to the regional stress field so long as the fault is located within an active area. Thus, in any given active area, existing faults will accommodate nearly all the brittle shear deformation. In the present model, this accommodation is partly through seismogenic slip (Figs. 1, 10), and partly through aseismic slip. The seismogenic slip is controlled by the dynamic moduli,

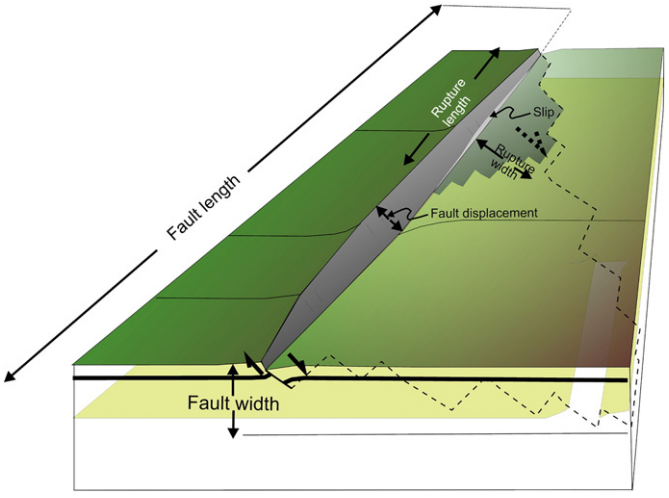

Fig. 10. Schematic illustration of fault growth through accumulation of seismic and aseismic slips. Length is strike dimension and width is dip dimension. Normally, only a part of a fault ruptures during a seismic or aseismic slip. The ratio between the fault length and maximum displacement is generally much smaller than the ratio between the rupture length and slip during individual slip events (cf. Fig. 1).

whereas the aseismic slip is mostly controlled by the static moduli. Since the static moduli is commonly one-tenth of the dynamic moduli, and the difference may be much greater between the fault core and innermost part of the damage zone (which control the static displacement), on the one hand, and the outer part of the damage zone, on the other hand, the static (long-term) rupture length–slip ratio is commonly of the order of 10^2-times the fault length–displacement ratio. In this model, part of the aseismic slip is thus due to adjustment of the dynamic, short-term rupture length–slip ratio to the static, long-term fault length–displacement ratio.

This model indicates that much of the shear strain is accommodated through fault displacement rather than through increasing fault length. All faults of course have finite lengths (Figs. 1, 10). But it follows from the common power-law length distribution of faults that most faults in any population are short in relation to the longest fault (Fig. 2). The present results (Figs. 5, 6), as well as other studies of faults (e.g., Walsh et al., 2002), indicate that displacement can accumulate on a fault during rupture events while the fault strike-dimension increases very little or not at all. To explore further how this happens, the following points related to the mechanics of faulting should be mentioned:

1. Fault slip occurs in response to stress concentration. The slip relaxes the driving shear stress that has concentrated at and around the fault before the slip. Following the slip all bending stresses in the walls of the fault along its flat-elliptical slip profile (Figs. 1, 10; Gudmundsson, 2011; Yeats et al., 1996) gradually become relaxed.
2. It follows from the power-law size distribution of fracture lengths in general (Fig. 2; Mohajeri and Gudmundsson, 2012; Turcotte, 1997) that most co-seismic slips in a fault zone are associated with ruptures that are much smaller than the dimensions of the fault zone as a whole (Figs. 1, 10). 'Small' here refers to both the strike dimension and the dip dimension of the ruptures in relation to the same dimensions of the fault zones within which the ruptures occur. The damage zone and fault core of an existing fault zone are much easier to rupture than the 'intact' host rock, so that for most co-seismic slips in a fault zone there is no tendency to increase the strike or dip dimensions of the fault zone as a whole.
3. Even for a large co-seismic ruptures, there is normally little tendency for a fault that has reached a certain length to continue to grow laterally. This follows because it requires much more energy to propagate the lateral ends into the host rock and rupture it rather than dissipate the energy through slip within the already existing fault zone. Thus, it is the energy available (Eq. (9)) to drive the slip that determines its size. But it is also the general elastic energy (strain energy and work; cf. Gudmundsson, 2012) that determines how large the strike dimension of the fault zone can become.
4. The energy available during co-seismic rupture is related to the work done on the fault zone. When the fault-zone boundaries move as a result of plate-tectonic loading, there is work done on the fault zone by its surroundings. This work increases the internal energy of the fault zone. This internal energy, partly stored as strain energy, together with the work associated with the movements of the fault-zone boundaries during rupture are the main energy sources available for driving the rupture propagation (cf. Gudmundsson, 2012).
5. An active fault zone with a breccia/gouge fault core and highly fractured damage zone (Fig. 8) has a very low long-term shear strength. The short-term strength relates to the intrinsic shear strength of the fault rocks, as well as to notches and jogs, asperities, that may temporarily lock the fault. The long-term strength of the fault, however, is commonly low and as soon as the yield strength is reached the fault can flow as a ductile or plastic material. This low strength makes many, perhaps most, faults weak (e.g., Zoback, 1991; Zoback et al., 2011). The accumulation of displacement along a fault of a given length is thus analogous to plastic flow; so long as the yield stress or strength is reached, the flow can continue. That faults are analogous to plastic yield follows directly from the main fault criterion, namely the Coulomb-criterion — and also from the Modified Griffith version of that criterion (Eq. (8)). The Coulomb criterion was originally derived for granular (plastic) materials and may be regarded as a generalisation (with mean stress or depth taken into account) of the well-known Tresca criterion for plastic yield (Chen, 2008; Gudmundsson, 2011).

8. Summary and conclusions

The difference between the short-term co-seismic rupture length–slip ratios, on the one hand, and the long-term length–displacement ratios of fault zones, on the other, has been known for many years. Little attempt, however, has been made to explain these differences in terms of mechanics of faulting. Here we propose an explanation of the difference between these ratios in terms of a general model on fault growth. The main conclusions of this paper may be summarised as follows:

- Co-seismic rupture length–slip ratios are commonly of the order of 10^{3-4}. This means that for a measured maximum seismogenic slip of 1 m, the strike dimension or length of the associated earthquake rupture would commonly be from one to tens of kilometres.
- Fault length–displacement ratios are commonly of the order of 10^{1-2}. This means that for a maximum measured displacement of 10 m, the strike dimension or length of the associated fault would commonly be from a fraction of a kilometre to several kilometres. For both co-seismic ruptures and faults the slips/displacements refer to the maximum values, which are commonly somewhere near the centre of the rupture/fault (Figs. 1, 10).
- New data on slips and lengths of 19 co-seismic ruptures and displacements and lengths of 7 faults on eastern the flanks of the volcano Etna, Italy, are presented. Most of the co-seismic and displacement data are from the same faults, and nearly all the faults dissect the same Holocene lava flows, so that the mechanical properties of the rocks that the faults dissect are generally similar. Most of the faults are normal faults.
- The lengths of the 19 co-seismic ruptures range from 100 m to 6500 m (average 3657 m), and the slips range from 0.03 m to 1.08 m (average of 0.31 m). The length–slip ratios range from 1333 to 87,500, with an average of 19,595.
- The lengths of the 7 faults range from 1150 m to 12,950 m (average 6341 m), and the displacements range from 8 m to 190 m (average 73 m). The length–displacement ratios range from 42 to 362, with an average of 130. It follows that the average rupture–slip ratio is about 150-times larger than the average length–displacement ratio.
- We propose a conceptual model whereby the large differences between the length–slip and the length–displacement ratios are partly explained by the difference in the dynamic and static Young's modulus of the fault zones. For a given fault zone, dynamic modulus may be 10^{1-2}-times larger than the static modulus, particularly close to and at the surface where most slip and displacement measurements are made. More specifically, we suggest that, commonly, it is the dynamics modulus of the outer damage zone that controls the length–slip ratios whereas the static modulus of the inner damage zone and the core controls the length–displacement ratio.
- In this model, part of the common aseismic slip (slow earthquakes, creep) in fault zones is due to adjustment of the short-term seismogenic length–slip ratio to the long-term (and partly aseismic) length–displacement ratio. The long-term fault displacement is regarded as analogous to plastic flow, and the long-term displacement can be very large so long as sufficient shear stress concentrates on the fault.
- Faults may be regarded as elastic inclusions, that is, rock bodies with mechanical properties (of the core and damage zone) that differ from those of the host rock. When subject to loading (stress, displacement, pressure) all inclusion concentrate stresses and modify the local

stress field. Consequently, faults tend to concentrate stresses and remain active even if they are not optimally orientated with reference to the regional stress field. Active faults continue to accumulate displacement while their lateral growth tends to come to an end early during their lifetimes. If follows that the length–displacement ratio of the fault may gradually decrease so long as it remains active.

Acknowledgements

We thank Francoise Bergerat and Shigekazu Kusomoto for very helpful comments that improved the paper.

References

Ambraseys, N.N., Jackson, J.A., 1998. Faulting associated with historical and recent earthquakes in the eastern Mediterranean region. Geophysical Journal International 133, 390–406.
Bell, F.G., 2000. Engineering Properties of Rocks, 4th ed. Blackwell, Oxford.
Biasi, G.P., Weldon, R.J., 2006. Estimating surface rupture length and magnitude of paleoearthquakes from point measurements of rupture displacement. Bulletin of the Seismological Society of America 96, 1612–1623.
Bonilla, M.G., Mark, R.K., Lienkaemper, J.J., 1984. Statistical relations among earthquake magnitude, surface rupture lengths, and surface fault displacements. Bulletin of the Seismological Society of America 74 (2379–2411), 1984.
Broberg, K.B., 1999. Cracks and Fracture. Academic Press, London.
Bruhn, R.L., Parry, W.T., Yonkee, W.A., Tompson, T., 1994. Fracturing and hydrothermal alteration in normal fault zones. Pure and Applied Geophysics 142, 609–644.
Caine, J.S., Evans, J.P., Forster, C.B., 1995. Fault zone architecture and permeability structure. Geology 24, 1025–1028.
Chen, W.F., 2008. Limit Analysis and Soil Plasticity. J. Ross, Fort Lauderdale, F.L.
Clark, R.M., Cox, S.J.D., 1996. A modern regression approach to determining fault displacement–scaling relationships. Journal of Structural Geology 18 (147–152), 1996.
Clauset, A., Chalizi, R.C., Newman, M.E.J., 2009. Power-law distributions in empirical data. Society for Industrial and Applied Mathematics 51, 661–703.
Cowie, P.A., Scholz, C.H., 1992. Displacement–length scaling relationships for faults: data synthesis and discussion. Journal of Structural Geology 14, 1149–1156.
De Guidi, G., Scudero, S., Gresta, S., 2012. New insights into the local crust structure of Mt. Etna volcano from seismological and morphotectonic data. Journal of Volcanology and Geothermal Research 223–224, 83–92. http://dx.doi.org/10.1016/j.jvolgeores.2012.02.001.
Eshelby, J.D., 1957. The determination of the elastic field of an ellipsoidal inclusion, and related problems. Proceedings of the Royal Society of London A 241, 376–396.
Faulkner, D.R., Mitchell, T.M., Healy, D., Heap, M.J., 2006. Slip on 'weak' fault by the rotation of regional stress in the fracture damage zone. Nature 444, 922–925.
Fjaer, E., 2009. Static and dynamic moduli of weak sandstones. Geophysics 74, WA103–WA112. http://dx.doi.org/10.1190/1.3052113.
Forslund, T., Gudmundsson, A., 1992. Structure of Tertiary and Pleistocene normal faults in Iceland. Tectonics 11, 57–68.
Galehouse, J.S., Lienkaemper, J.J., 2003. Inferences drawn from two decades of alignment array measurements of creep on faults in the San Francisco Bay region. Bulletin of the Seismological Society of America 93, 2415–2433.
Giampiccolo, E., D'Amico, S., Patane, D., Gresta, S., 2007. Attenuation and source parameters of shallow microearthquakes at Mt. Etna Volcano, Italy. Bulletin of the Seismological Society of America 97, 184–197. http://dx.doi.org/10.1785/0120050252.
Gillespie, P.A., Walsh, J.J., Waterson, J., 1992. Limitations of dimension and displacement data from single faults and the consequences for data analysis and interpretation. Journal of Structural Geology 14, 1157–1172.
Goodman, R.E., 1989. Introduction to Rock Mechanics, 2nd ed. Wiley, New York.
Gresta, S., Patanè, G., 1983a. Changes in b values before the Etnean eruption of March–August 1983. Pure and Applied Geophysics 121, 903–912.
Gresta, S., Patanè, G., 1983b. Variation of b values before the Etnean eruption of March 1981. 121, 287–295.
Gudmundsson, A., 2000. Fracture dimensions, displacements and fluid transport. Journal of Structural Geology 22, 1221–1231.
Gudmundsson, A., 2004. Effects of Young's modulus on fault displacement. Comptes Rendus Geoscience 336, 85–92.
Gudmundsson, A., 2005. Effects of mechanical layering on the development of normal faults and dykes in Iceland. Geodinamica Acta 18, 11–30.
Gudmundsson, A., 2007. Infrastructure and evolution of ocean-ridge discontinuities in Iceland. Journal of Geodynamics 43, 6–29.
Gudmundsson, A., 2011. Rock Fractures in Geological Processes. Cambridge University Press, Cambridge.
Gudmundsson, A., 2012. Strengths and strain energies of volcanic edifices: implications for eruptions, collapse calderas, and landslides. Natural Hazards and Earth System Sciences 12, 2241–2258.
Gudmundsson, A., Mohajeri, N., 2013. Relations between the scaling exponents, entropies, and energies of fracture networks. Bulletin of the Geological Society of France 184, 377–387.
Gudmundsson, A., Simmenes, T.H., Larsen, B., Philipp, S.L., 2010. Effects of internal structure and local stresses on fracture propagation, deflection, and arrest in fault zones. Journal of Structural Geology 32, 1643–1655.
Heap, M.J., Vinciguerra, S., Meredith, P.G., 2009. The evolution of elastic moduli with increasing crack damage during cyclic stressing of a basalt from Mt. Etna volcano. Tectonophysics 471, 153–160. http://dx.doi.org/10.1016/j.tecto.2008.10.004.
Heuze, F.E., 1980. Scale effects in the determination of rock mass strength and deformability. Rock Mechanics 12, 167–192.
Hickman, S., Zoback, M., Ellsworth, W., Boness, N., Malin, P., Roecker, S., Thurber, C., 2007. Structure and properties of the San Andreas Fault in central California: recent results from the SAFOD experiments. Scientific Drilling (1), 29–32 (Special Issue).
Hoek, E., 2000. Practical Rock Engineering. http://www.rockscience.com.
Imposa, S., 2008. Focal parameters of seismic sources during the 1981 and 1983 eruption at Mt. Etna volcano (Sicily, Italy). Environmental Geology 55, 1061–1073.
Jordan, T.H., et al., 2003. Living on an active earth: perspectives on earthquake science. National Research Council of the National Academies.The National Academic Press, Washington D.C.
Kagan, Y.Y., 2002. Aftershock zone scaling. Bulletin of the Seismological Society of America 92, 641–655.
Kanamori, H., Anderson, D.L., 1975. Theoretical basis of some empirical relations in seismology. Bulletin of the Seismological Society of America 65, 1073–1095.
Kasahara, K., 1981. Earthquake Mechanics. Cambridge University Press, Cambridge.
Larsen, B., Gudmundsson, A., 2010. Linking of fractures in layered rocks: implications for permeability. Tectonophysics 492, 108–120.
Ledbetter, H., 1993. Dynamic vs. static Young's moduli: a case study. Materials Science and Engineering A165, L9–L10.
Leonard, M., 2010. Earthquake fault scaling: self-consistent relating of rupture length, width, average displacement, and moment release. Bulletin of the Seismological Society of America 100, 1971–1988.
Li, H., van der Woerd, J., Sun, Z., Si, J., Tapponnier, P., Pan, J., Liu, D., Chevalier, M.L., 2012. Co-seismic and cumulative offsets of the recent earthquakes along the Karakax left-lateral strike-slip fault in western Tibet. Gondwana Research 21, 64–87.
Lockner, D.A., Byerlee, J.D., Kuksenko, V., Ponomarev, A., Sidori, A., 1991. Quasi-static fault growth and shear fracture energy in granite. Nature 350, 39–42.
Manighetti, I., Zigone, D., Campillo, M., Cotton, F., 2009. Self-similarity of the largest-scale segmentation of the faults: implications for earthquake behaviour. Earth and Planetary Science Letters 288, 370–381.
McFarland, F.S., Lienkaemper, J.J., Caskey, S.J., 2009. Data from theodolite measurements of creep rates on San Francisco Bay region faults, California, 1979–2009. USGS Open-file Report 2009–1119. (http://pubs.usgs.gov/of/2009/1119/).
Mohajeri, N., Gudmundsson, A., 2012. Entropies and scaling exponents of street and fracture networks. Entropy 14, 800–833.
Monaco, C., De Guidi, G., Catalano, S., Ferlito, C., Tortorici, G., Tortorici, L., 2008. La carta morfotettonica dell'Etna. Rendiconti Online della Società Geologica Italiana 1, 217–218.
Nicol, A., Walsh, J.J., Watterson, J., Childs, C., 1996. The shapes, major axis orientations and displacement patterns of fault surfaces. Journal of Structural Geology 18, 235–248.
Nur, A., 1974. Tectonophysics: the study of relations between deformation and forces in the earth. Advances in Rock Mechanics, vol. 1, part A. U.S. National Academy of Sciences, Washington D.C., pp. 243–317.
Patanè, G., Coco, G., Corrao, M., Imposa, S., Montalto, A., 1995. Source parameters of seismic events at Mount Etna volcano, Italy, during the outburst of the 1991–1993 eruption. Physics of the Earth and Planetary Interiors 89, 149–162.
Pavlides, S., Caputo, R., 2004. Magnitude versus faults' surface parameters: quantitative relationships from the Aegean Region. Tectonophysics 380, 159–188.
Peng, Z., Gomberg, J., 2010. An integrated perspective of the continuum between earthquakes and slow-slip phenomena. Nature Geoscience 3, 599–607.
Peng, A., Johnson, A.M., 1972. Crack growth and faulting in cylindrical specimens of the Chelmsford Granite. International Journal of Rock Mechanics and Mining Science 9, 37–86.
Priest, S.D., 1993. Discontinuity Analysis for Rock Engineering. Chapman and Hall, London.
Rolandone, F., Burgmann, R., Agnew, D.C., Johanson, I.A., Templeton, D.C., d'Alessio, M.A., Titus, S.J., DeMets, C., Tikoff, B., 2008. Aseismic slip and fault-normal strain along the central creeping section of the San Andreas fault. Geophysical Research Letters 35, L14305. http://dx.doi.org/10.1029/2008GL034437.
Romanowicz, B., Ruff, L.J., 2002. On moment-length scaling of large strike slip earthquakes and the strength of faults. Geophysical Research Letters 29 (12). http://dx.doi.org/10.1029/2001GL014479.
Savin, G.N., 1961. Stress Concentrations Around Holes. Pergamon, London.
Schlische, R.W., Young, S.S., Ackermann, R.V., Gupta, A., 1996. Geometry and scaling relations of a population of very small rift-related normal faults. Geology 24, 683–686.
Scholz, C.H., 2002. The Mechanics of Earthquakes and Faulting, 2nd ed. Cambridge University Press, Cambridge.
Shipton, Z.K., Cowie, P.A., 2001. Damage zone and slip-surface evolution over μm to km scales in high-porosity Navajo sandstone, Utah. Journal of Structural Geology 23, 1825–1844.
Sibson, R.H., 1990. Rupture nucleation on unfavorably oriented faults. Bulletin of the Seismological Society of America 80, 1580–1604.
Sleep, N.H., Blanpied, M., 1992. Creep, compaction and weak rheology of major faults. Nature 359, 687–692.
Smith, W.D., 1981. The b-value as an earthquake precursor. Nature 289, 136–139.
Stein, S., Wysession, M., 2003. An Introduction to Seismology, Earthquakes, and the Earth Structure. Blackwell, Oxford.
Tada, H., Paris, P.C., Irwin, G.R., 2000. The Stress Analysis of Cracks Handbook, 3rd ed. ASME Press, New York.

Turcotte, D.L., 1997. Fractals and Chaos in Geology and Geophysics, 2nd ed. Cambridge University Press, Cambridge.
Turcotte, D.L., Shcherbakov, R., Rundle, J.B., 2007. Complexity and earthquakes. In: Kanamori, H. (Ed.), Treatise on Geophysics, vol. 4. Elsevier, Amsterdam, pp. 675–700 (Chap. 23).
Vermilye, J.M., Scholz, C.H., 1998. The process zone: a microstructural view of fault zones. Journal of Geophysical Research 103, 12,223–12,237.
Walsh, J.J., Nicol, A., Childs, C., 2002. An alternative model for the growth of faults. Journal of Structural Geology 24, 1669–1675.
Wells, D., Coppersmith, K., 1994. New empirical relationships among magnitude, rupture length, rupture width, rupture area, and surface displacement. Bulletin of the Seismological Society of America 84, 974–1002.
Yeats, R.S., 2012. Active Faults of the World. Cambridge University Press, Cambridge.
Yeats, R.S., Sieh, K., Allen, C.R., 1996. The Geology of Earthquakes. Oxford University Press, Oxford.
Zoback, M.D., 1991. State of stress and crustal deformation along weak transform faults. Philosophical Transactions of the Royal Society of London 337, 141–150.
Zoback, M.D., Hickman, S., Ellsworth, W., the SAFOD science team, 2011. Scientific drilling into the San Andreas fault zone — an overview of SAFOD's first five years. Scientific Drilling 11, 14–28.